Improving the study of proton transfers between amino acid sidechains in solution: choosing appropriate DFT functionals and avoiding hidden pitfalls.

Pedro J. Silva[1], Marta A. S. Perez[2], Natércia F. Brás[2], Pedro A. Fernandes[2] and M. J. Ramos[2]*

[1]REQUIMTE, Fac. de Ciências da Saúde, Univ. Fernando Pessoa, Rua Carlos da Maia, 296, 4200-150 Porto-Portugal

[2]REQUIMTE, Faculdade de Ciências do Porto, Rua do Campo Alegre, 687, 4169-007 Porto – Portugal

*mjramos@fc.up.pt

Abstract: We have studied the influence of implicit solvent models, inclusion of explicit water molecules, inclusion of vibrational effects, and density functionals on the quality of the predicted pK_a of small amino acid sidechain models. We found that the inclusion of vibrational effects and explicit water molecules is crucial to improve the correlation between the computed and the experimental values. However, achieving convergence of the results requires the addition of too many explicit water molecules, which generate new problems related to the presence of multiple minima in the potential energy surface. It thus appears that a satisfactory *ab initio* prediction of amino acid sidechain pK_a will require methods that fully sample the potential energy surface in the presence of large solvation shells, while at the same time computing vibrational contributions to the enthalpy and entropy of the system under study in all points of that surface. Pending development of efficient algorithms for those computations, we strongly suggest that whenever abnormal protonation states are found in a computational study the reaction profile should be computed under the each of the different protonation micro-states by constraining the relevant N-H or O-H bonds, in order to avoid artifacts inherent to the complex nature of the factors contributing to the pK_a.

Keywords: DFT; benchmarking; Acid/base reactions; amino acid sidechains

Introduction

The ubiquitous presence of protonation/deprotonation steps in the catalytic mechanisms of organic and biochemical reactions is responsible for the experimentally observed large effects of pH on many reaction rates. A good theoretical description of these reaction mechanisms therefore depends on the ability to predict accurately the solution pK_a of the reacting functional groups. Several protocols for computational determination of pK_a have been developed by several authors [1-6]. They all rely on the determination of gas-phase reaction energies, followed by computation of solvation energies of the basic and acidic forms of the molecular species under study using implicit solvent models[1-3,5,6] or the Poisson equation [4], in the presence [2,3,5,6] or absence [1,4,6] of a few explicit water molecules. The computed energy values are then converted to pK_a using appropriate thermodynamic cycles. Clearly, the quality of the results obtained critically depends on the accuracy of the individual computations performed in each step of the protocol, and this is reflected, e.g., on the different correlations obtained between computed and experimental values obtained for different classes of acids [7].We have recently performed a thorough benchmarking study of the ability of 51 density functionals to accurately describe the gas phase behavior of large amino acid models [8]. However, to the best of our knowledge, no systematic study of the influence of each factor on the quality of the predicted pK_a values has been performed to date.

In this report we describe the influence of: the implicit solvent model, inclusion of explicit water molecules, neglect of vibrational effects, and density functional used on the quality of predicted pK_a. We found that the inclusion of vibrational effects and explicit water molecules is crucial to improve the correlation between the computed and the experimental values. However, achieving convergence of the results requires the addition of too many explicit water molecules, which introduce new problems related to the presence of multiple minima in the potential energy surface. A satisfactory resolution of this problem will likely require long quantum dynamics simulations in the presence of large solvation shells.

Computational methods

The geometries of every molecule described were optimized at the MP2 level and with each of the tested density functionals. Autogenerated delocalized coordinates[9] were used in geometry optimizations performed with a medium-sized basis set, 6-31+G(d), as increasing the basis sets to triple-ζ quality gives very small additional corrections to the geometries while dramatically increasing the computational cost [10-12]. Accurate DFT energies of the optimized geometries obtained with each density functional were then calculated using the same functional with several triple-ζ quality basis sets: 6-311+G(d,p), 6-311+G(2d,p), 6-311+G(2d,2p), and 6-311+G(3d,2p). We used three GGA functionals (PBE96[13,14], PBEPW91[13,14] and PW91[13]), eight hybrid-GGA functionals (B3LYP[15,16,17], B3PW91[13,15], B97-1[18], B97-2[19], BHHLYP (50% HF exchange + plus 50% B88[20] exchange, with LYP correlation), PBE0[21], PBE1PW91[13,14], and X3LYP[22]), three meta-GGA functionals (TPSS[23,24], TPSSm[25], and M06-L[28]) and four meta-hybrid GGA functionals (TPSSh[26], M06[27], M06-2X[27] and M06-HF[29]). Computations involving CCSD(T), the B97-1, B97-2 and the M06 and TPSS families of functionals were performed with Gamess(US)[30]. All other computations were performed with the Firefly[31] quantum chemistry package. CCSD(T) and MP2 single-point energies were computed on the MP2 geometries using 6-31+G(d), aug-cc-pVDZ and aug-cc-pVTZ basis sets and extrapolated to the complete basis set limit as described by Schwenke [32] (for CCSD(T) level) or Truhlar [33,34] (at the MP2 level). Comparison of these values to experimental free energies of protonation required the inclusion of the contribution of H^+ to the Gibbs free energy of the protonation reactions ($G_{gas,H+}$= -6.28 kcal.mol^{-1} at 298 K and 1 atm) and the evaluation of zero-point and thermal effects on these geometries (computed from the MP2/6-31+G(d) frequencies using a scaling factor of 0.967 [35]).

Since the computation of gas phase Gibbs free energies through any computational method entails the determination of the electronic energies and zero-point/vibrational energies (ZPVE) of each reactant and

each product, the performance of a functional depends not only on the accuracy of the computed electronic energies but also on the quality of the vibrational frequencies provided by the method. In this work, we decided to focus on the electronic reaction energies *only*, to prevent spurious results arising from mutual cancellation of errors in energy/ZPVE and because no ZPVE scaling factors are available for many of the method/basis set combinations tested. Electronic-only basicities were computed as E_{acid}-E_{base}. DFT solvation energies were computed using the Polarizable Continuum Model[36] implemented in each package (D-PCM[37,38] in Firefly and C-PCM[39,40] in Gamess (US)). Average DFT solvation energies were used as estimates of MP2 solvation energies.

Guanidine was selected as model for arginine acidities, aspartate/glutamate and lysine were modeled as acetate and methylamine (respectively). Methanethiol was chosen to represent the cysteine sidechain, and phenol as tyrosine model. Histidine was modeled as methylimidazole. Both δ-deprotonated and ε-deprotonated forms of methylimidazole were computed; all methods predicted the δ-deprotonated form to lie slightly lower in energy than the ε-deprotonated form. The average value for these protonations was used in all method comparisons, to avoid lending more weight to the histidine protonation vs. other aminoacids.

Results and Discussion

I. Benchmarking selected density-functionals in the gas phase

The energies of the selected set of model reactions range from -223.6 kcal.mol^{-1} to -364.1 kcal.mol^{-1} at the CCSD(T) /CBS // MP2/6-31+G(d) level (Table 1). Energies predicted by MP2/CBS lie a few kcal.mol^{-1} above CCSD(T)/CBS in all instances. Both theory levels agree very well with experimental results (Table 1), and can therefore be used as appropriate benchmarks for the density functional theory computations. Interestingly, MP2/CBS agrees the most with experiment in the reactions involving a protonated and a neutral species, whereas CCSD(T) outperforms MP2/CBS in reactions involving a neutral and an anionic species.

Table 1: Computed gas-phase protonation energies of the amino acid side chain models. All values in kcal.mol^{-1}. Bolded data in parentheses include zero-point energy, enthalpic and entropic contributions at 298.15 K computed at the MP2/6-31+G(d) level and can be directly compared to the experimental ΔG values.

	Amino acid	MP2/CBS	CCSD(T)/CBS	Experimental value
i)	Arginine	-239.9 (**-226.6**)	-242.6 (**-229.3**)	-226.9[41]
ii)	Aspartate	-352.6 (**-338.3**)	-356.1 (**-341.8**)	-341.4± 1.2[42]
iii)	Cysteine	-360.5 (**-348.3**)	-364.1 (**-351.8**)	-350.6 ± 2.0[42]
iv)	Histidine (δ-protonation)	-234.1 (**-218.4**)	-237.4 (**-221.7**)	-220.1 ± 2.0[41]
v)	Histidine (ε-protonation)	-234.5 (**-219.6**)	-237.8 (**-222.9**)	
vi)	Lysine	-221.6(**-206.2**)	-223.6 (**-208.2**)	-206.6 ± 0.5[41]
vii)	Tyrosine	-354.4 (**-340.1**)	-358.1 (**-343.8**)	-342.9 ± 1.4[42]

Density functional theory generally afforded geometries in very good agreement with MP2 geometries (root-mean-squared errors were most often below 0.02 Å). Large differences between functionals were only observed for the protonated arginine model: TPSS, TPSSm, PBE96, PBEPW91 and PW91 agree almost perfectly with the MP2 geometry (RMSD < 0.015 Å), whereas BHHLYP places the hydrogens closer to the plane defined by the heavier atoms than the MP2 reference (RMSD = 0.077 Å); other functionals show RMSD vs. MP2 between 0.02 and 0.05 Å. All tested functionals correctly predict the relative ordering of the gas-phase reaction energies in this test set as dictated by experiment and CCSD(T)/CBS (with the exception of PBE96, PBEPW91 and PW91, which erroneously predict the protonation of the tyrosine model to be marginally less favourable than that of the aspartate model). The reaction energies obtained with the DFT functionals are generally over-estimated relative to the CCSD(T)/CBS energies; B97-2 and BHHLYP are the major exceptions to this trend, as they under-estimate all protonation energies (see Supporting Information).

II. Computing basicities in solution

Gas phase benchmark results are not directly applicable to the computation of basicities in solution because the amount of stabilization provided by the solvent depends on the amount of delocalized charge in the tested molecule. We therefore computed the reaction energies in solution for each of the reaction with every density functional, using the Polarizable Continuum Model. As expected from simple charge considerations, the inclusion of solvent strongly favoured the protonation of neutral species and disfavoured the protonation of charged (anionic) species and therefore dramatically reduced the large spread of protonation energies, from -220 kcal.mol^{-1}/-360 kcal.mol^{-1} in gas phase to -280 kcal.mol^{-1}/-306 kcal.mol^{-1} in solution. However, the computed values correlate very poorly with the experimental trends: for example, aspartate is still predicted to be more basic than histidine (though much less so than in gas phase), irrespective of the Polarizable Continuum Model used (either C-PCM[39,40] or D-PCM[36] using an escaped charge compensation scheme[37,38]) (Figure 1). Inclusion of zero-

point and thermal effects does not improve these results: the correlation coefficients between computed and experimental values barely change from R^2=0.013 to 0.025 (C-PCM) and from R^2=0.123 to 0.135 (D-PCM).

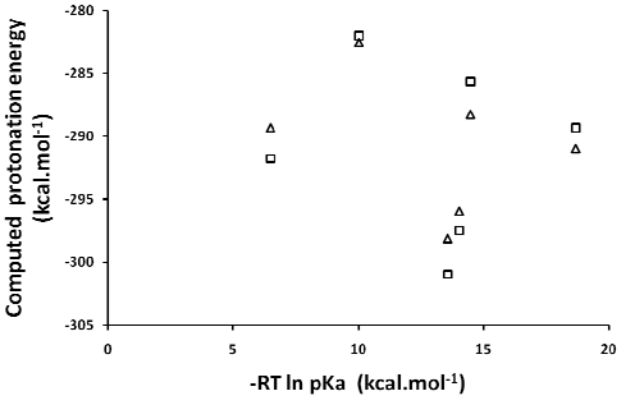

Figure 1: Computed MP2/CBS protonation energy in solution vs. experiment. (Δ): solvation energies computed with D-PCM. (□) solvation energies computed with C-PCM. ZPVE and thermal effects not included. Protonation energies are E_{acid}-E_{base} and do not include H^+ solvation.

Such poor performance of the PCM models conflicts with the usually good estimates of solvation energies they are able to provide[43]. Further analysis showed that this problem arises from the neglect of solvent-dependent stabilizing effects of a non-electrostatic nature, since the inclusion of two explicit water molecules to the MP2 optimization of every system (or three water molecules in the case of the lysine and arginine models) greatly improves the correlation with experiment, though *only* upon addition of zero-point and thermal effects. Under these conditions, the correlation coefficients increase to R^2=0.399 (C-PCM) and R^2=0.578 (D-PCM), which (although encouraging) is still far below chemical accuracy (Figure 2). Our attempts at systematic improvement of these results by expanding the micro-solvation spheres were thwarted by the onset of difficulties regarding conformational sampling. This occurs because as the number of water molecules around the solute increases, so does the number of water-water interactions. In these small solute-water clusters the change in number of hydrogen-

bonds between the solute and the water as the solute is protonated often causes a dramatic reorganization of the water-water hydrogen bonds in the cluster, leading to large geometric between the acidic and basic forms of the solute and misleading energy differences, that depend not only on the protonation energy itself, but also on the different regions of the potential energy surface of the solvent micro-cluster analysed in each protonation state.

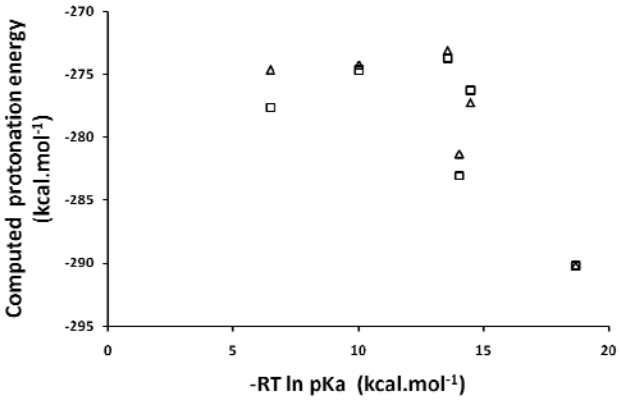

Figure 2: Computed MP2/CBS protonation energy in solution vs. experiment, including explicit water molecules. (Δ): including solvation energies computed with D-PCM. (□) including solvation energies computed with C-PCM. ZPVE and thermal effects are included. Protonation energies are E_{acid}-E_{base} and do not include H^+ solvation.

The results above clearly show that attaining chemical accuracy in the *ab initio* prediction of pKa is prevented by the need to include: a large solvation shell around the solutes, zero-point and vibrational effects throughout the potential energy surface, and sufficient conformational sampling needed to take into account each of the many local minima present in the potential energy surface. However, such large *ab initio* quantum dynamics studies still lie beyond the reach of current computational technologies. It is therefore useful to identify the density functional(s) that more closely approach the MP2 results in micro-solvated systems for eventual application in DFT-based quantum dynamics.

We compared the MP2 micro-solvation behavior of the amino acid systems with density-functional theory by performing additional geometry optimizations with the explicitly solvated systems with each density functional, followed by computation of high quality single-point energies in a Polarizable Continuum Model. In all cases, the hydrogen bond lengths remain quite constant among methods, but due to the rotational flexibility of the added water molecules the agreement between the obtained geometries and the MP2 geometries is substantially lower than observed in the water-free models. Root-mean squared deviations range from 0.17 Å (average value obtained with B3LYP or X3LYP) to 0.39 Å (average value obtained with M06). We found that, whereas the precise implementation of the Polarizable Continuum Model (either D-PCM or C-PCM) strongly affected the magnitude of its effect on the reaction energies, within each implementation its effect was mostly independent of the precise geometry of the models (standard deviation of the continuum contribution to the reaction energies < 0.7 kcal.mol^{-1}). Comparisons of DFT-derived reaction energies with the MP2/CBS benchmark in these micro-solvated systems are presented in Table 6. Although most functionals afforded errors above 1.4 kcal.mol^{-1} (≈1 pKa unit), and two (B97-2 and BHHLYP) yielded large errors > 5 kcal.mol^{-1}, three functionals (M06, M06-2X and PW91) yielded results very similar to the MP2 benchmark. Further analysis shows that these surprisingly large errors arise mostly from systematic under-estimation (M06-HF, PBE0, PBE96, PW91, PBEPW91 and PBE1PW91) or over-estimation (all other functionals, except M06-2X) of reaction energies. Many of these systematic errors cancel when the deprotonation energies of the amino acid models are compared with each other. Table 3 depicts the mean unsigned errors for the *differences* in reaction energies (which we call *relative* reaction energies) for all 6×5/2 reactions obtained by coupling any two acid/base pairs tested for each method, with the 6-311+G(3d,2p) basis sets. BHHLYP and B97-2 now emerge clearly as the best overall choices (closely followed by TPSSh). To help the user in the choice of functional, Table 4 presents the best functionals (and corresponding errors) for each of the individual proton transfers between aminoacid sidechains.

Table 2: Mean Unsigned Errors in the computation of absolute reaction energies with micro-solvated models using the 6-311+G(3d,2p) basis set. All values in kcal.mol^{-1}. ZPVE not included. Error values below 1.5 kcal.mol^{-1} are highlighted in bold.

		MUE vs. MP2/CBS (gas phase optimized)	MUE vs. MP2/CBS (PCM optimized)
PBE96	GGA	2.11±1.90	±
PBEPW91	GGA	2.01±1.83	±
PW91	GGA	**1.34±1.13**	±
B3LYP	hybrid-GGA	1.90±1.27	1.63±2.06
B3PW91	hybrid-GGA	3.61±1.35	2.54±2.33
B97-1	hybrid-GGA	2.50±1.42	±
B97-2	hybrid-GGA	5.15±1.11	±
BHHLYP	hybrid-GGA	5.24±1.12	±
PBE0	hybrid-GGA	2.30±1.27	±
PBE1PW91	hybrid-GGA	1.96±1.74	±
X3LYP	hybrid-GGA	1.56±1.17	±
TPSS	meta-GGA	2.15±1.11	±
TPSSm	meta-GGA	2.31±1.15	±
M06	meta-hybrid-GGA	**1.34±0.89**	±
M06-2X	meta-hybrid-GGA	**1.34±1.44**	±
M06-HF	meta-hybrid-GGA	2.81±2.32	±
M06-L	meta-hybrid-GGA	3.71±1.69	±
TPSSh	meta-hybrid-GGA	3.22±1.11	±

Table 3: Mean Unsigned Errors in the computation of reaction energy *differences* with micro-solvated models using the 6-311+G(3d,2p) basis set. All values in kcal.mol^{-1}. ZPVE not included. Error values below 1.5 kcal.mol^{-1} are highlighted in bold.

		MUE vs. MP2/CBS (gas-phase optimized)	MUE vs. MP2/CBS (PCM optimized)
PBE96	GGA	2.92±1.76	2.68±2.48
PBEPW91	GGA	2.86±1.73	3.70±2.46
PW91	GGA	1.97±1.23	3.92±2.42
B3LYP	hybrid-GGA	1.52±0.99	**1.46±0.91**
B3PW91	hybrid-GGA	1.64±1.00	1.75±1.13
B97-1	hybrid-GGA	1.84±1.21	2.42±1.41
B97-2	hybrid-GGA	**1.35±0.83**	2.98±2.51
BHHLYP	hybrid-GGA	**1.20±1.07**	**1.41±0.89**
PBE0	hybrid-GGA	1.99±1.25	3.17±1.99
PBE1PW91	hybrid-GGA	2.78±1.69	3.91±2.59
X3LYP	hybrid-GGA	**1.47±0.99**	1.62±0.98
TPSS	meta-GGA	**1.50±1.20**	1.70±1.26
TPSSm	meta-GGA	**1.49±1.20**	2.68±1.79
M06	meta-hybrid-GGA	1.77±1.15	2.15±1.8
M06-2X	meta-hybrid-GGA	2.19±1.95	2.44±2.80
M06-HF	meta-hybrid-GGA	2.68±1.97	3.23±2.90
M06-L	meta-hybrid-GGA	1.97±1.40	2.24±1.51
TPSSh	meta-hybrid-GGA	**1.23±1.01**	**1.46±1.34**

Table 4: Suggested DFT functionals for the study of reactions involving proton transfer between micro-solvated amino acid sidechains. Absolute errors (kcal.mol^{-1}) (DFT/6-311+G(3d,2p) vs. MP2/CBS) shown in parentheses.

	Arg deprotonation	Asp/Glu deprotonation	Cys deprotonation	His deprotonation	Lys deprotonation
Asp/Glu protonation	TPSSh and TPSSm (<0.1)				
Cys protonation	PW91(<0.2)	B3LYP, TPSS and TPSSm (<0.1)			
His protonation	X3LYP (0.4)	M06-L (<0.1)	M06-2X (<0.9)		
Lys protonation	TPSSh (<0.2)	B3PW91, B97-1 and TPSS (<0.1)	X3LYP (<0.1)	B97-2 (0.4)	
Tyr protonation	M06-L (<0.2)	BHHLYP (<0.1)	M06-2X (<0.3)	BHHLYP and M06-HF (<0.4)	M06 (<0.2)

Conclusions

It is clear from the results that, although in most cases a very satisfactory agreement between density functional theory and MP2 is found, the accuracy of the computed MP2 protonation energies in solution is still far from perfect, even with explicit micro-solvation of the chemical systems under study (Figure 2). Preliminary trials revealed that improvement is unlikely to be achieved simply by a small increase in the number of explicit water molecules. Very large increases on the size of the solvent cluster, on the other hand, quickly takes the problem out of reach of pure QM methodologies, and further compounds

the problems due to the very large number of possible minima in the potential energy surface. The large effect of the zero-point and thermal effects on the quality of the correlations should also be kept in mind whenever proton transfer between amino acid side chains is studied, as these effects may reverse the computed relative basicities (e.g. using only electronic energies lysine is predicted to be more acidic than histidine, whereas the inclusion of ZPVE and thermal effects results in the prediction of higher acidity of histidin relative to lysine). Since the computation of these vibrational contributions from the molecular hessian is only possible at stationary points, the full description of the free energy surface landscape must necessarily involve other methods of estimating entropic contributions, such as quntum dynamics simulations.

These confounding effects are probably at play in a number of theoretical studies that predict abnormal protonation behaviours, such as the predictions of a neutral aspartate/neutral histidine dyad instead of an anionic aspartate/cationic histidine)[44,45,46], the proposal of an anionic histidine/neutral aspartate dyad in the reaction mechanism of Ca^{2+}-dependent phospholipase[47], or the prediction of neutral arginine/aspartic acid pairs instead of arginine/aspartate salt bridges[48]. We strongly suggest that whenever abnormal protonation states are found in a computational study the reaction profile should be computed under the each of the different protonation micro-states by constraining the relevant N-H or O-H bonds. This strategy will provide a fuller understanding of the influence of each specific state of the relevant amino acid dyad on the reaction mechanism and avoid artifacts inherent to the complex nature of the factors contributing to the basicities of amino acid sidechains.

SUPPORTING INFORMATION Geometries of every described molecule optimized with each density functional and with MP2, as well as their electronic energies with different basis sets.

REFERENCES

1 C. O. da Silva, E. C. da Silva, M. A. C. Nascimento, J. Phys. Chem. A (1999) 103, 11194-11199

2 K. R. Adam, J. Phys. Chem. A (2002) 106, 11963-11972

3 J. R. Pliego Jr. , J. M. Riveros, J. Phys. Chem. A (2002) 106, 7434-7439

4 M. Schmidt am Busch, E. W. Knapp, ChemPhysChem (2004) 5, 1513-1524

5 C. P. Kelly, C. J. Cramer, D. G. Truhlar, J. Phys. Chem. A (2006) 110, 2493-2499

6 J. Ho, M. L. Coote, Theor. Chem. Acc. (2010) 125, 3-21

7 M. Peräkylä, Phys. Chem. Chem. Phys. (1999) 1, 5643-5647

8 N. F. Brás, M. A. S. Perez, P.A. Fernandes, P. J. Silva, M.J. Ramos, J. Chem. Theor. Comp. submitted

9 J. Baker, A. Kessi, B. Delley, J. Chem. Phys. 105 (1996) 192

10 P.E.M. Siegbahn, L. Eriksson, F. Himo, M. Pavlov, J. Phys. Chem. B. , 102 (1998) 10622.

11 P.A. Fernandes, M.J. Ramos, J. Am. Chem. Soc. , 125 (2003) 6311

12 K.E. Riley, B. T. Op't Holt, K. M. Merz Jr. , J. Chem. Theory Comput. , 3 (2007) 407

13 J.P. Perdew, "Unified Theory of Exchange and Correlation Beyond the Local Density Approximation. " In Electronic Structure of Solids '91 pp 11-20; Ziesche, P. , Eschig, H. , Eds. ; Akademie Verlag: Berlin, Germany, 1991

14 J.P. Perdew, K. Burke, M. Ernzerhof, Phys. Rev. Lett. , 77 (1996) 3865

15 A. D. Becke, J. Chem. Phys. I, 98 (1993) 5648

16 C. Lee, W. Yang, R. Parr, J. Phys. Rev. B, 37 (1998) 785

17 R. W. Hertwig, W. Koch, J. Comp. Chem. , 16 (1995) 576.

18 F. A. Hamprecht, A. J. Cohen, D. J. Tozer, N.C. Handy, J. Chem. Phys. , 109 (1998) 6264

19 P.J. Wilson, T. J. Bradley, D. J. Tozer, J. Chem. Phys.,115 (2001) 9233

20 A. D. Becke, Phys. Rev. A, 38 (1988) 3098

21 C. Adamo, V. Barone, J. Chem. Phys. , 110 (1999) 6158

22 X. Xu, Q. Zhang, R. P. Muller, W. A. Goddard, J. Chem. Phys. , 122 (2005) 014105

23 J. P. Perdew, J. Tao, V. N. Staroverov, G. E. Scuseria, Phys. Rev. Lett. , 91 (2003) 146401

24 J. P. Perdew, J. Tao, V. N. Staroverov, G. E. Scuseria, J. Chem. Phys. , 120 (2004) 6898

25 J. P. Perdew, A. Ruzsinszky, J. Tao, G. I. Csonka, G. E. Scuseria, Phys. Rev. A, 76 (2007) 042506

26 V. N. Staroverov, G. E. Scuseria, J. Tao, J. P. Perdew, J. Chem. Phys. , 119(2003) 12129; erratum in J. Chem. Phys. , 121, 11507

27 Y. Zhao, D. G. Truhlar, Theoret. Chem. Acc. , 120 (2008) 215

28 Y. Zhao, D. G. Truhlar, J. Chem. Phys. , 125 (2006) 194101

29 Y. Zhao, D. G. Truhlar, J. Phys. Chem. A , 110 (2006) 13126

30 M.W. Schmidt, K.K. Baldridge, J. A. Boatz, S.T. Elbert, M.S. Gordon, J.J. Jensen, S. Koseki, N. Matsunaga, K.A. Nguyen, S. Su, T.L. Windus, M. Dupuis, J.A. Montgomery, J. Comput. Chem. , 14 (1993) 1347

31 A. A. Granovsky, PC GAMESS/Firefly version 7.0, http://classic.chem.msu.su/gran/gamess/index.html

32 D.W. Schwenke, J. Chem. Phys. **122** (2005) 014107

33 D. G. Truhlar, Chem. Phys. Lett. , 294 (1998) 45

34 Y. Zhao, D. G. Truhlar, J. Phys. Chem. A, 109 (2005) 6624

35 J. P. Merrick, D. Moran, L. Radom, J. Phys. Chem. A (207) 111, 11683-11700

36 J. Tomasi, M. Persico, Chem. Rev. (1994) 94, 2027-2094

37 B. Mennucci, J. Tomasi J. Chem. Phys. (1997) 106, 5151-5158

38 M. Cossi, B. Mennucci, J. Pitarch, J. Tomasi J. Comput. Chem. (1998) 19, 833-846

39 V. Barone, M. Cossi J. Phys. Chem. A (1998) 102, 1995-2001

40 M. Cossi, N. Rega, G. Scalmani, V. Barone J. Comput. Chem. (2003) 24, 669-681

41 E. P. Hunter, S. G. Lias, J. Phys. Chem. Ref. Data (1998) 27, 413-656

42 P. Linstrom, W. Mallard, Eds. *NIST Chemistry WebBook, NIST Standard Reference Database Number 69*; National Institute of Standards and Technology: Gaithersburg, MD, 2003; http://webbook.nist.gov

43 V. Barone, M. Cossi, J. Tomasi, J. Chem. Phys. (1997) 107, 3210-3221

44 P. C. Gómez and L. F. Pacios, Chem. Phys. Phys. Chem. (2005) 7, 1374-1381

45 J. Wang, H. Dong , H. Li and H. He ,J. Phys. Chem. B (2005) 109, 18664-18672

46 B. Schiøtt, Chem. Commun. (2004), 498-499

47 M. Leopoldini, N. Russo and M. Toscano, J. Phys. Chem. B (2010) 114, 11584-11593

48 P. I. Nagy, P.W. Erhardt, J. Phys. Chem. B (2010) 114, 16436-16442